




## Research paper

# Combined effects of elevated CO<sub>2</sub> and warmer temperature on limitations to photosynthesis and carbon sequestration in yellow birch

Lei Wang<sup>1,2</sup>, Jinping Zheng<sup>1,3</sup>, Gerong Wang<sup>1,3</sup> and Qing-Lai Dang<sup>1,4</sup> 

<sup>1</sup>Faculty of Natural Resources Management, Lakehead University, 955 Oliver Road, Thunder Bay, Ontario P7B 5E1, Canada; <sup>2</sup>Department of Biotechnology, College of Biotechnology, Jiangsu University of Science and Technology, Zhenjiang, Jiangsu 212003, China; <sup>3</sup>Forestry College, Beihua University, 3999 Binjiang East Road, Jilin, Jilin 132013, China; <sup>4</sup>Corresponding author (qdang@lakeheadu.ca)

Received August 4, 2022; accepted September 30, 2022; handling Editor David Tissue

**Elevated CO<sub>2</sub> and warmer temperature occur simultaneously under the current climate change. However, their combined effects on the photosynthetic traits in boreal trees are not well understood. This study investigated the morphological and photosynthetic responses of yellow birch (*Betula alleghaniensis* Britt.) to a combined treatment of CO<sub>2</sub> and temperature (ambient, ACT (400 μmol mol<sup>-1</sup> CO<sub>2</sub> and current temperature) vs elevated, ECT (750 μmol mol<sup>-1</sup> CO<sub>2</sub> and current +4 °C temperature)). It was found that ECT significantly reduced leaf-area based photosynthetic rate ( $A_n$ ), maximum Rubisco carboxylation rate ( $V_{cmax}$ ), photosynthetic electron transport rate ( $J_{max}$ ), leaf nitrogen concentration, respiration and mesophyll conductance. There were two interesting findings: first, the primary mechanism of photosynthetic limitation shifted from Ribulose-1,5-bisphosphate (RuBP) carboxylation (related to  $V_{cmax}$ ) to RuBP regeneration (related to  $J_{max}$ ) in response to ECT, leading to decreased transition point ( $C_{i-t}$  and  $A_{n-t}$ ) from RuBP carboxylation to regeneration; second, the increase in total leaf area in response to ECT more than compensated for the downregulation of leaf-area based photosynthesis, leading to greater biomass in ECT than in ACT. We proposed a new protocol for evaluating photosynthetic limitations by comparing the relative relationship between the transition point ( $C_{i-t}$  and  $A_{n-t}$ ) and the photosynthetic rate at growth CO<sub>2</sub> ( $C_{i-g}$  and  $A_{n-g}$ ). Furthermore, we found that  $J_{max}$  (RuBP regeneration) was the primary limitation to  $A_n$  under ECT.**

**Keywords:** *Betula alleghaniensis* Britt, global warming, leaf area, mechanisms of photosynthetic limitation.

## Introduction

Greenhouse gas emissions are the leading cause of climate change, and CO<sub>2</sub> in particular is one of the largest contributors to global warming, comprising almost one-half of the total negative impact (IPCC 2021). Recent studies have found that chloroplast precursors protein (TT3.2) transduces heat signals from the plasma membrane to chloroplasts, and chloroplasts may also participate in responding to temperature fluctuations and thermotolerance (Zhang et al. 2022). Climate warming will be coupled with the rise of CO<sub>2</sub> in the atmosphere in the foreseeable future (IPCC 2021). Plants, therefore, will have to adjust from the current CO<sub>2</sub> and temperature conditions

to future elevated CO<sub>2</sub> and higher temperature, including a possible increase in extreme weather events (Slot et al. 2021). Understanding the morphological and physiological responses of plants to the combined effects of elevated CO<sub>2</sub> and temperature is the basis for predicting the impacts of climate change on vegetation and developing adaptation strategies (Tcherkez et al. 2017).

Elevated CO<sub>2</sub> generally leads to reductions in photosynthetic capacity ( $V_{cmax}$  and  $J_{max}$ ) and leaf nitrogen concentration (Birami et al. 2020, Ainsworth and Long, 2021). It is generally believed that photosynthetic downregulation optimizes the coordination of various components in the photosynthetic system to

Table 1. Definition of acronyms.

Acronyms	Definitions	Unit
$A/C_i$	Net photosynthesis rate versus CO <sub>2</sub> response curve	—
ACE	Apparent carboxylation efficiency	—
ACT	Treatment of ambient 400 $\mu\text{mol mol}^{-1}$ CO <sub>2</sub> and ambient temperature	—
$A_n$	Net photosynthesis rate	$\mu\text{mol m}^{-2} \text{s}^{-1}$
$A_{n\text{-ACT}400}$	$A_n$ of ACT-treated seedlings at growth 400 $\mu\text{mol mol}^{-1}$ CO <sub>2</sub>	$\mu\text{mol m}^{-2} \text{s}^{-1}$
$A_{n\text{-ECT}750}$	$A_n$ of ECT-treated seedlings at growth 750 $\mu\text{mol mol}^{-1}$ CO <sub>2</sub>	$\mu\text{mol m}^{-2} \text{s}^{-1}$
$A_{n\text{-g}}$	$A_n$ at growth CO <sub>2</sub> concentration	$\mu\text{mol mol}^{-1}$
$A_{n\text{-t}}$	$A_n$ at the transition point between RuBP carboxylation to regeneration limitation	$\mu\text{mol m}^{-2} \text{s}^{-1}$
$A_{n\text{-g}}/A_{n\text{-t}}$	Ratio of $A_{n\text{-g}}$ and $A_{n\text{-t}}$	—
$C_a$	Ambient CO <sub>2</sub> concentration	$\mu\text{mol mol}^{-1}$
$\text{CCP}_{aci}$	CO <sub>2</sub> compensation point from $A/C_i$ curve	$\mu\text{mol mol}^{-1}$
$C_i$	Intercellular CO <sub>2</sub> concentration	$\mu\text{mol mol}^{-1}$
$C_i^*$	Intercellular CO <sub>2</sub> compensation point	$\mu\text{mol mol}^{-1}$
$C_{i\text{-t}}$	$C_i$ at the transition point between RuBP carboxylation to regeneration limitation	$\mu\text{mol mol}^{-1}$
$C_i/C_a$	Intercellular ( $C_i$ ) to ambient ( $C_a$ ) CO <sub>2</sub> concentration ratio	—
$C_{i\text{-g}}$	$C_i$ at growth CO <sub>2</sub> concentration	$\mu\text{mol mol}^{-1}$
$C_{i\text{-g}}/C_{i\text{-t}}$	Ratio of $C_{i\text{-g}}$ and $C_{i\text{-t}}$	—
ECT	Treatment of 750 $\mu\text{mol mol}^{-1}$ CO <sub>2</sub> and elevated temperature (ambient +4 °C)	—
$C_{i\text{-ACT}400}$	$C_i$ of ACT-treated seedlings at growth 400 $\mu\text{mol mol}^{-1}$ CO <sub>2</sub>	$\mu\text{mol mol}^{-1}$
$C_{i\text{-ECT}750}$	$C_i$ of ECT-treated seedlings at growth 750 $\mu\text{mol mol}^{-1}$ CO <sub>2</sub>	$\mu\text{mol mol}^{-1}$
$\Phi\text{PHII}$	Photochemical efficiency of photosystem II	—
$g_m$	Mesophyll conductance	$\text{mol m}^{-2} \text{s}^{-1}$
$J_c$	Electron transport to carboxylation	$\mu\text{mol m}^{-2} \text{s}^{-1}$
$J_o$	Electron transport to oxygenation	$\mu\text{mol m}^{-2} \text{s}^{-1}$
$J_{\text{max}}$	Maximum photosynthetic electron transport rate	$\mu\text{mol m}^{-2} \text{s}^{-1}$
LMR	Leaf mass ratio	—
$N_{\text{area}}$	Leaf N content based on leaf area	$\text{g m}^{-2}$
$N_{\text{mass}}$	Leaf N concentration-based mass	$\text{mg g}^{-1}$
$R_d$	Daytime respiration	$\mu\text{mol m}^{-2} \text{s}^{-1}$
SLA	Specific leaf area	$\text{g m}^{-2}$
SMR	Stem mass ratio	—
$V_{\text{cmax}}$	Maximum rate of RuBP carboxylation	$\mu\text{mol m}^{-2} \text{s}^{-1}$

maximize carbon gains (Ross et al. 2020). The optimization of nitrogen distribution is the biochemical basis of photosynthetic downregulation, and nitrogen supply determines the final status of photosynthetic downregulation (Yin et al. 2019). However, results on how elevated CO<sub>2</sub> impacts the relationship between photosynthetic capacity and foliar nitrogen concentration are inconsistent in the literature (Kurepin et al. 2018, Chavan et al. 2019). While increasing nitrogen supply generally eliminates or reduces the degree of photosynthetic downregulation (Yin et al. 2019), some studies have found that photosynthetic downregulation in response to elevated CO<sub>2</sub> is not correlated with leaf nitrogen concentration or nitrogen supply (Pastore et al. 2019, Silva-Pérez et al. 2020). Results on how temperature affects photosynthetic responses to elevated CO<sub>2</sub> are also inconsistent in the literature. Some researchers find that those responses are independent of growth temperature and moisture conditions (Salazar-Parra et al. 2015), while others report that temperature is a key factor influencing different components of the photosynthetic system and affects photosynthetic response to elevated CO<sub>2</sub> (Mathan et al. 2021).

Assessing photosynthetic acclimation to elevated CO<sub>2</sub> involves the elucidation of the specific processes or components that limit photosynthesis. According to the FvCB model, limitations to photosynthesis in C3 plants primarily include RuBP carboxylation (indicated by  $V_{\text{cmax}}$ ), RuBP regeneration (indicated by  $J_{\text{max}}$ ) and triosephosphate utilization (TPU) (Busch and Sage 2017). The RuBP carboxylation is generally the primary limitation to photosynthesis under normal light and ambient CO<sub>2</sub> concentrations. As CO<sub>2</sub> supply increases, however, RuBP regeneration can become the primary limiting factor to photosynthesis (related to  $J_{\text{max}}$ ), but TPU is rarely a primary limitation to photosynthesis under normal environmental conditions (Kumarathunge et al. 2019). As the CO<sub>2</sub> concentration in the atmosphere continues to increase,  $J_{\text{max}}$  may play a more important role in regulating photosynthesis in the future before the photosynthetic apparatus is fully acclimated to the prevailing CO<sub>2</sub> (Suzuki et al. 2021). However, the change in primary photosynthetic limitations has not received sufficient attention in studies on photosynthetic acclimation to rising CO<sub>2</sub>. The transition point ( $C_{i\text{-t}}$  and  $A_{n\text{-t}}$ , see Table 1 for

details) from RuBP carboxylation limitation to RuBP regeneration limitation has been considered to be insignificant since the photosynthetic rate under the current CO<sub>2</sub> cannot reach  $A_{n-t}$  (Kumarathunge et al. 2019). Little is known about factors influencing the transition point (Busch and Sage, 2017). When RuBP regeneration becomes the primary limiting factor under elevated CO<sub>2</sub>, the photosynthetic rate should be greater than  $A_{n-t}$ , but there is a paucity of such information in the literature. Zhou et al. (2015) find that the changes in  $J_{\max}/V_{\text{cmax}}$  ratio can reflect the changes in photosynthetic limitations and are related to nitrogen partitioning between RuBP carboxylation and regeneration. Therefore, the transition point may represent the photosynthetic co-limitation by  $J_{\max}$  and  $V_{\text{cmax}}$  and is related to photosynthetic acclimation to CO<sub>2</sub> (Noyce et al. 2019). Co-limitation represents the optimal allocation of nitrogen between the biochemical and photochemical apparatuses (Lambers and Oliveira 2019). Therefore, plants tend to reallocate resources in responses to changes in environmental conditions so that photosynthesis operates near a  $C_i$  where photosynthesis is co-limited by  $J_{\max}$  and  $V_{\text{cmax}}$  under the average conditions. Elevated CO<sub>2</sub> generally increases the  $J_{\max}/V_{\text{cmax}}$  ratio (Smith and Keenan, 2020). By contrast, warmer temperatures tend to decrease the  $J_{\max}/V_{\text{cmax}}$  ratio (Kumarathunge et al. 2019). However, there are no consistent conclusions on the combined effect of elevated CO<sub>2</sub> and warmer temperature on  $J_{\max}/V_{\text{cmax}}$  ratio in the literature. Some studies report that elevated temperature and elevated CO<sub>2</sub> synergistically improve photosynthesis, growth and stress resistance (Apgaua et al. 2019), while others suggest that there are no significant interactive effects between the two factors on photosynthesis (Dusenge et al. 2020). Therefore, further studies are warranted on the combined effects of warmer temperature and elevated CO<sub>2</sub> on plant physiology and growth (Jayawardena et al. 2019).

Yellow birch (*Betula alleghaniensis* Britt.) is a common deciduous tree species, in the north temperate zone, with a medium growth rate (Delagrangue et al. 2004). Yellow birch produces not only high-quality wood but also bioactive substances, which can be used in the food, pharmaceutical and cosmetic industries (Lavoie and Stevanovic 2005). Yellow birch may be particularly vulnerable to global warming due to its shallower root system (Cox and Zhu 2003). This study examined how the photosynthetic characteristics and growth of yellow birch seedlings responded to the combination treatment of elevated CO<sub>2</sub> and warmer temperature. We have tested the following three hypotheses: elevated CO<sub>2</sub> in combination with a warmer temperature would (i) shift the primary limitation to photosynthesis, (ii) alter the transition point between Rubisco limitation and RuBP regeneration limitation and (iii) increase total leaf area if photosynthetic downregulation occurs. Past research has indicated that the trends of responses are consistent among enclosure studies on tree seedlings, open top chamber studies on larger trees in the field and free-air CO<sub>2</sub> enrichment

experiments, although the magnitude of the responses can be different (Long et al. 2004, Ainsworth and Long 2005). Thus, the performance of seedlings can be a good indicator of tree's response (Anderson-Teixeira et al. 2013, Inoue et al. 2019). Studies on seedlings in controlled environment are particularly suitable for examining the mechanisms of responses to multiple factors because several factors can be manipulated simultaneously.

## Materials and methods

### Plant materials and treatments

Yellow birch seeds were collected from 10 natural trees of the same population on Changbai Mountain (42.12°N and 127.51°E) in China. The seeds were sown in germination trays filled with vermiculite and peat moss (1:1 in v:v) at the Lakehead University research greenhouse (Thunder Bay campus). The seedlings were individually transplanted into 3.5-l pots filled with a mixture of peat moss and vermiculite (1:1 v/v) 18 days after the completion of germination. The seedlings were watered every 2 days to the drip point and were fertilized twice a week using a fertilizer solution (N-P-K 50–60–150  $\mu\text{mol mol}^{-1}$ ) with a micronutrient. The day/night temperatures during the germination were set at 25/16 °C, and the photoperiod was 16 h.

Two [CO<sub>2</sub>]-temperature combination treatments were used in this experiment: ACT, ambient CO<sub>2</sub> concentration (400  $\mu\text{mol mol}^{-1}$ ) and current temperature (25/16 °C, day/night); and ECT, elevated CO<sub>2</sub> concentration (750  $\mu\text{mol mol}^{-1}$ ) and current +4 °C temperature (29/20 °C day/night). Each treatment combination was replicated twice in two separate greenhouses. The temperature and photoperiod in the ACT emulated those of the growing season (June–September) at the seed origin. The photoperiod regime in the ECT was identical to that of the ACT treatment. High-pressure sodium lamps (P.L. Systems, Grimsby, ON, Canada) were used to extend the natural photoperiod when the natural day-length was shorter than the photoperiod being emulated. The environmental conditions in all the greenhouses were controlled using an Argus Titan Environment-control system (Argus Control Systems Ltd, Vancouver, BC, Canada). The daily temperature in each greenhouse was changed at 3-h intervals to emulate the natural daily variations at the seed origin, and the photoperiod and temperature settings were adjusted weekly to emulate the seasonal pattern.

### Gas exchange measurements and parameters

Following 2 months of treatments, three seedlings were randomly selected from each replicate of each treatment (six seedlings were measured in total for each treatment) and  $A/C_i$  curves on the first fully expanded leaf were measured at 400, 300, 200, 150, 100, 50, 400, 500, 750, 900,



Table 2. Student's *t*-test *P*-values for the effects of CO<sub>2</sub>-temperature combination treatment (ACT: 400 μmol mol<sup>-1</sup> [CO<sub>2</sub>] and current temperature vs ECT: 750 μmol mol<sup>-1</sup> [CO<sub>2</sub>] and current +4 °C temperature) on biomass and morphological traits, foliar nitrogen concentration and leaf-area-based photosynthetic variables (leaf VAR) of yellow birch seedlings.

Biomass/morph	<i>P</i> -value	Leaf VAR	<i>P</i> -value	Leaf VAR	<i>P</i> -value
Biomass	<b>&lt;0.001</b>	$V_{cmax}$	0.13	$R_l$	<b>&lt;0.001</b>
RMR	0.257	$J_{max}$	<b>&lt;0.001</b>	$g_m$	<b>&lt;0.001</b>
SMR	<b>&lt;0.001</b>	$J_{max}/V_{cmax}$	<b>&lt;0.001</b>	$R_d$	<b>0.023</b>
LMR	<b>0.024</b>	$V_{cmax}/N_{area}$	<b>0.013</b>	$J_c$	<b>&lt;0.001</b>
SLA	0.965	$C_{i-t}$	<b>0.019</b>	$J_o$	<b>&lt;0.001</b>
Root/shoot ratio	<b>0.015</b>	$A_{n-t}$	<b>&lt;0.001</b>	$J_c/J_o$	0.077
Leaf area	<b>&lt;0.001</b>	CCP <sub>aci</sub>	0.057	$A_{n-g}$	<b>0.005</b>
Height	<b>&lt;0.001</b>	$C_i^*$	0.598	$A_{n-g}/A_{n-t}$	<b>&lt;0.001</b>
$N_{area}$	<b>&lt;0.001</b>	ACE	<b>0.014</b>	$C_{i-g}/C_{i-t}$	<b>&lt;0.001</b>
$N_{mass}$	<b>0.005</b>	ΦPHII	<b>0.007</b>	$N_{leaf}$	<b>0.014</b>

Note: Biomass: total seedling biomass; RMR: root mass ratio; SLA: leaf mass ratio;  $N_{area}$ : leaf N per unit area;  $N_{mass}$ : leaf N concentration;  $V_{cmax}$ : maximum rate of Rubisco carboxylation;  $J_{max}$ : maximum of photosynthetic electron transport rate;  $J_{max}/V_{cmax}$ : the ratio of  $J_{max}$  to  $V_{cmax}$ ;  $V_{cmax}/N_{area}$ : max carboxylation per unit leaf N;  $C_{i-t}$ : intercellular [CO<sub>2</sub>] at the transition point from Rubisco limitation to RuBP regeneration limitation based on  $A/C_i$  curve;  $A_{n-t}$ : net photosynthesis rate at  $C_{i-t}$ ; CCP<sub>aci</sub>: CO<sub>2</sub> compensation point from  $A/C_i$  curve;  $C_i^*$ : intercellular CO<sub>2</sub> compensation point;  $R_l$ : photorespiration rate;  $g_m$ : mesophyll conductance;  $R_d$ : daytime respiration;  $J_c$ : electron transport to carboxylation;  $J_o$ : electron transport to oxygenation;  $J_c/J_o$ : ratio of  $J_c$  to  $J_o$ ;  $A_{n-g}$ : net photosynthesis rate at grow  $C_a$  which ECT treatment at 750 μmol mol<sup>-1</sup> ( $A_{n-ECT750}$ ) and ACT treatment at 400 μmol mol<sup>-1</sup> ( $A_{n-ACT400}$ );  $A_{n-g}/A_{n-t}$ : the ratio of  $A_{n-g}$  and  $A_{n-t}$ ;  $C_{i-g}/C_{i-t}$ : the ratio of  $C_i$  at grow  $C_a$  ( $C_{i-g}$ ) and  $C_{i-t}$ ;  $N_{leaf}$ : total N of the whole-plant leaf ( $N_{leaf} = N_{mass} \times \text{leaf mass, mg plant}^{-1}$ ). Significant effects ( $P \leq 0.05$ ) are printed in bold.

1100 and 1300 μmol mol<sup>-1</sup> CO<sub>2</sub> ( $C_a$ ) using a PP-Systems CIRAS-3 Portable Photosynthesis System equipped with a PLC3 Universal Leaf Cuvette with automatic climate control and a built-in CFM-3 Chlorophyll Fluorescence Module (PP Systems International, Inc., Amesbury, MA, USA). Other environmental conditions for the measurement were 25 °C air temperature, 800 μmol m<sup>-2</sup> s<sup>-1</sup> photosynthetically active radiation flux density (measured saturating PAR for photosynthesis was 600 μmol m<sup>-2</sup> s<sup>-1</sup>) and 50% relative humidity for both treatments. While measuring  $A/C_i$  curves at a common temperature for both treatments facilitates between-treatment comparisons and is consistent with the common practice in plant ecophysiology, the result can not reflect the effect of any thermos-acclimation that might have occurred. The maximum rate of RuBP carboxylation ( $V_{cmax}$ , μmol m<sup>-2</sup> s<sup>-1</sup>) and maximum rate of electron transport ( $J_{max}$ , μmol m<sup>-2</sup> s<sup>-1</sup>) were estimated using the Plantecophys fitaci function of the R package from  $A/C_i$  data (Duursma 2015). The initial slope of  $A/C_i$  curves was used as the apparent carboxylation efficiency (ACE) and the X-axis intercept of the  $A/C_i$  curve was used as an estimate of the CO<sub>2</sub> compensation point (CCP<sub>aci</sub>). The transition point ( $C_{i-t}$  and  $A_{n-t}$ ) between Rubisco limitation and RuBP regeneration limitation was obtained from the  $A/C_i$  curve using findCiTransition in the plantecophys R package (Duursma 2015).

The Laik script (200, 150, 100 and 50 μmol mol<sup>-1</sup> CO<sub>2</sub>, and PAR at 300, 150 and 75 μmol m<sup>-2</sup> s<sup>-1</sup>) measurements (Momayyezi and Guy 2017) were taken after the  $A/C_i$  measurements to estimate daytime respiration ( $R_d$ ) and intercellular CO<sub>2</sub> compensation point ( $C_i^*$ ; Farquhar et al. 1980). Chlorophyll fluorescence was measured using the built-in CFM-3 model of

the PP Systems CIRAS-3 system to calculate electron transport ( $J$ ). The variable  $J$  method was employed to calculate  $g_m$  (Peter et al. 1992), assuming that  $C_i^*$  equals to  $\Gamma^*$  (Momayyezi and Guy 2017).

The  $R_l$  and  $R_t$  were obtained as follows:

$$R_l = [J - 4(A_n + R_d)]/12,$$

$$R_t = R_d + R_l,$$

where  $R_l$  is the photorespiration rate and  $R_t$  denotes the total leaf respiration under the light. The  $J_c$  (electron transport to carboxylation) and  $J_o$  (electron transport to oxygenation) were calculated according to (Valentini et al. 1995, Tomeo and Rosenthal 2018), as follows:

$$J_c = [J + 8(A_n + R_d)]/3,$$

$$J_o = [J - 4(A_n + R_d)]2/3, \text{ respectively.}$$

Leaf-area based physiological variables were upscaled to the whole-tree level by multiplying the variables by the total leaf area of the tree (m<sup>2</sup> plant<sup>-1</sup>) (Jayawardena et al. 2019), whereas the total leaf nitrogen content per plant ( $N_{leaf}$ , mg plant<sup>-1</sup>) was calculated by multiplying  $N_{mass}$  (mg g<sup>-1</sup>) by the total leaf mass (g<sup>-1</sup>).

### Biomass and leaf nitrogen

At the completion of all the measurements, the seedling's total height was measured. All the seedlings were then harvested and the total leaf area per seedling was determined using a Regent WinFolia system (Regent Instruments Inc., Quebec City, QC, Canada). All the plant materials were then oven-dried at 75 °C for 48 h to obtain leaf biomass, stem and branch biomass and root biomass. Leaf nitrogen concentration was assayed using the dry combustion method using a CNS-2000 (LECO

Corp., St Joseph, MI, USA) by the Lakehead University Centre for Analytical Services. Leaf-area based nitrogen concentration ( $N_{area}$ , g m<sup>-2</sup>) was calculated by dividing the mass-based leaf nitrogen concentration ( $N_{mass}$ , mg g<sup>-1</sup>) by the specific leaf area.

### Statistical analyses

The effects of CO<sub>2</sub> and temperature combination treatment were tested using the Student's *t*-test. All data met the normality of distribution (tested via probability plots for residuals) and the homogeneity of variance (examined using scatter plots) assumptions. Principal component analysis (PCA) was applied to all the physiological and biomass parameters using the PCA function from the FactoMineR package. Correlation analyses were performed to examine the relationships between biomass,  $A_{n-t}$  and  $J_{max}$  and leaf area. All the analyses were performed using the R Package 4.0.6.

## Results

### Growth and leaf-level photosynthetic traits

The ECT significantly increased seedling biomass, total leaf area, height and shoot mass ratio but decreased the root/shoot ratio, leaf mass ratio and both area- and mass-based leaf nitrogen concentrations (Table 2, Figure 1). The ECT treatment significantly reduced  $J_{max}$  (maximum rate of photosynthetic electron transport rate),  $J_{max}/V_{cmax}$  ratio,  $J_{max}/N_{area}$  (maximum electron transport rate per unit leaf nitrogen),  $R_d$  (daytime respiration),  $R_i$  (photorespiration rate),  $A_{n-t}$  ( $A_n$  at the transition point ( $C_{i-t}$  and  $A_{n-t}$ ) from Rubisco limitation to RuBP regeneration limitation based on  $A/C_i$  curve),  $C_{i-t}$  (intercellular [CO<sub>2</sub>] at the transition point ( $C_{i-t}$  and  $A_{n-t}$ ) on  $A/C_i$  curve),  $\Phi_{PIII}$  (photochemical efficiency of photosystem II),  $J_c$  (electron transport to carboxylation),  $J_o$  (electron transport to oxygenation) and  $g_m$  (mesophyll conductance), but increased  $V_{cmax}/N_{area}$  (maximum rate of carboxylation per unit leaf nitrogen; Figure 2, Table 2) and had no significant effect on  $V_{cmax}$ ,  $C_i^*$  and  $J_c/J_o$  (Table 2).

### Biomass, leaf area, $J_{max}$ , $A_{n-t}$ impact source and sink relationship

The PCA revealed that the seedlings subjected to the ACT treatment tended to group the photosynthetic parameters (mainly affected by  $J_{max}$ ,  $A_{n-t}$  and  $R_i$ ) on the right ellipse of PC1, while the ECT-treated seedlings clustered toward the left ellipse of PC1 with the carbon sink parameters include biomass, leaf area and SMR (Figure 3). In addition, there is an inverse relationship between the parameters that greatly affect ECT and ACT because their arrows are close to 180 degrees in the PCA diagram (Figure 3), and the correlation analysis in Figure 4a and d shows similar results.

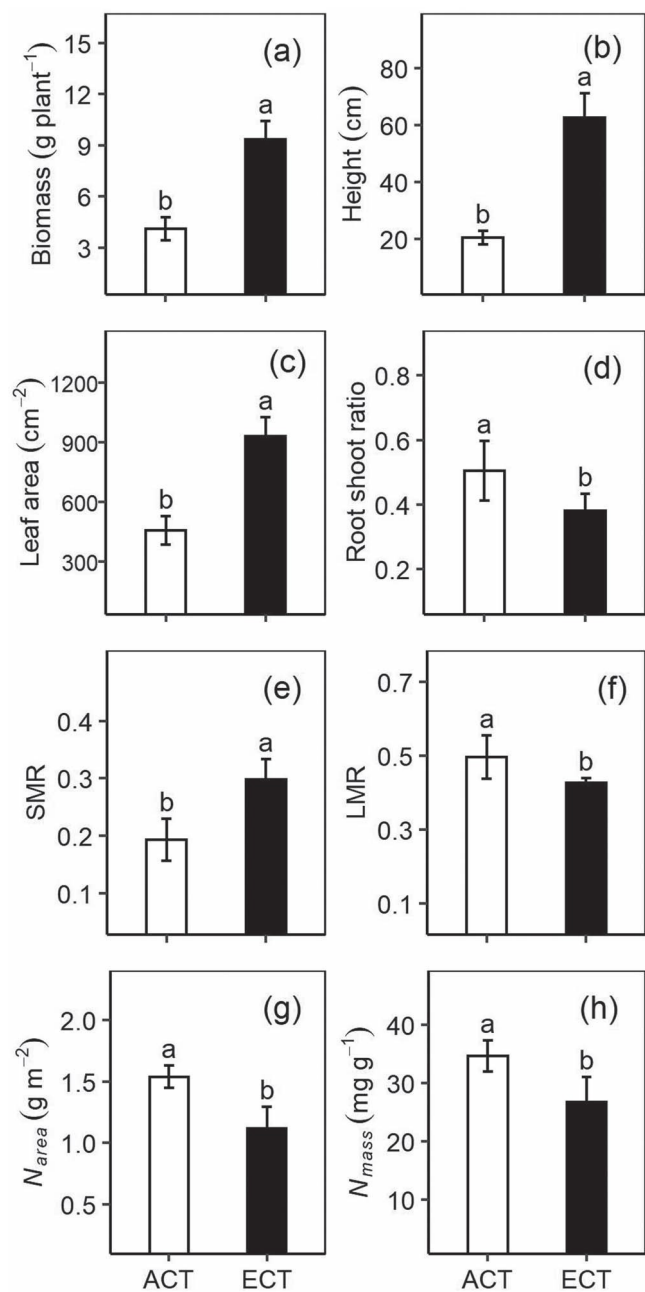


Figure 1. Effects of CO<sub>2</sub> and temperature combination (ACT: 400  $\mu\text{mol mol}^{-1}$  CO<sub>2</sub> and current temperature vs ECT: 750  $\mu\text{mol mol}^{-1}$  CO<sub>2</sub> and current temperature + 4 °C) on biomass and morphological traits of yellow birch seedlings: Biomass (a), Height (b), Leaf area (c), Root shoot ratio (d), SMR (e), leaf mass ratio (LMR) (f),  $N_{area}$  (area-based leaf N) (g) and  $N_{mass}$  (mass-based leaf N) (h). The seedlings were grown either under ACT (ambient 400  $\mu\text{mol mol}^{-1}$  CO<sub>2</sub> and current temperature) or ECT (750  $\mu\text{mol mol}^{-1}$  CO<sub>2</sub> and elevated temperature (ambient +4 °C)). Means ( $\pm$ SE,  $n = 6$ ) with different letters were significantly different from each other ( $P \leq 0.05$ ).

### Patterns and transition points ( $C_{i-t}$ and $A_{n-t}$ ) of $A/C_i$ curve

The ECT treatment significantly reduced the  $C_{i-t}$  and  $A_{n-t}$  values at the point of transition from RuBP carboxylation to RuBP

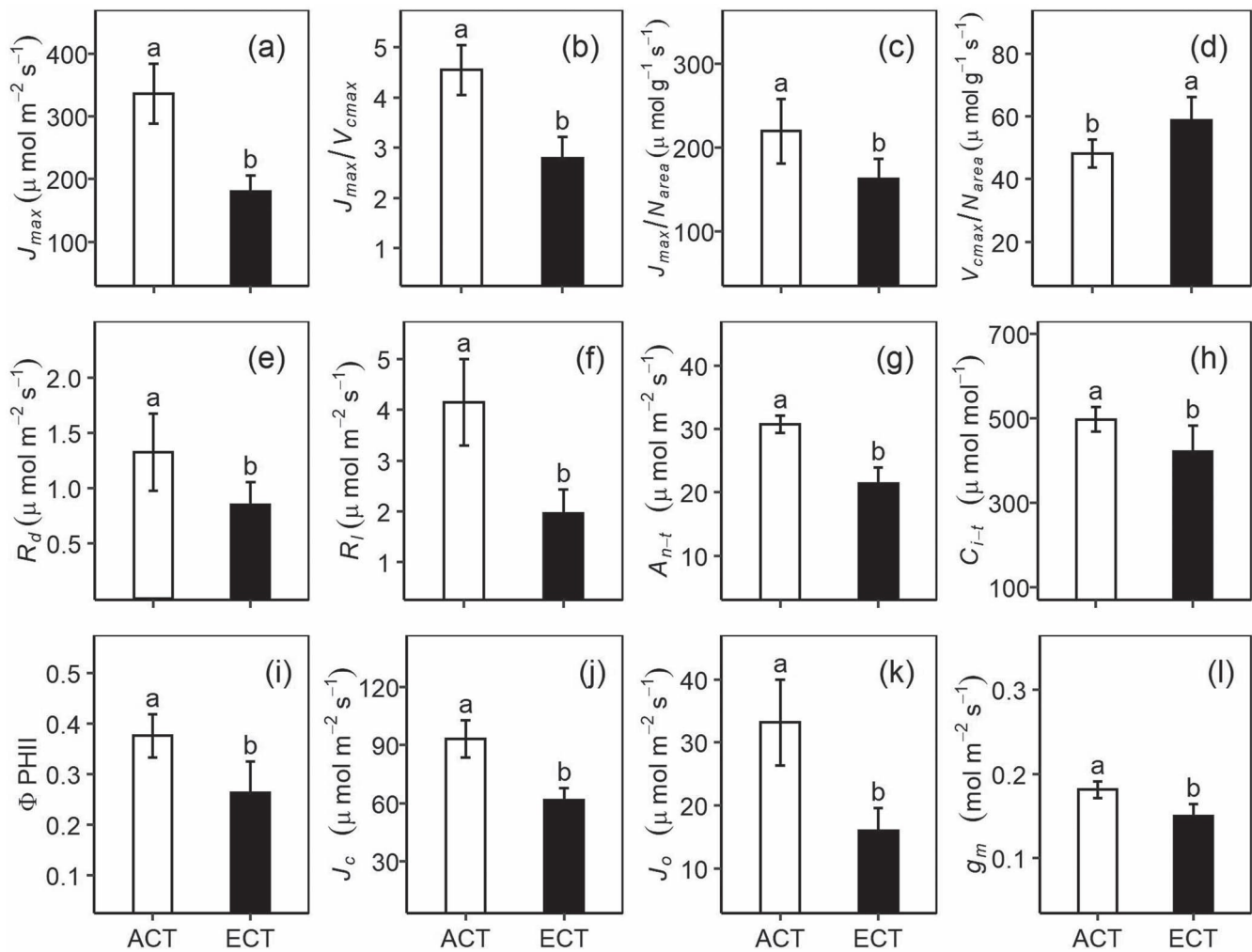


Figure 2. Effects of CT treatment on  $J_{max}$  (maximum rate of photosynthetic electron transport rate) (a),  $J_{max}/V_{cmax}$  ratio (b),  $J_{max}/N_{area}$  (maximum electron transport rate per unit leaf nitrogen) (c),  $V_{cmax}/N_{area}$  (maximum rate of carboxylation per unit leaf nitrogen) (d),  $R_d$  (daytime respiration) (e),  $R_l$  (photorespiration rate) (f),  $A_{n-t}$  ( $A_n$  at the transition point ( $C_{i-t}$ ,  $A_{n-t}$ ) from Rubisco limitation to RuBP regeneration limitation based on  $A/C_i$  curve) (g),  $C_{i-t}$  (intercellular  $[\text{CO}_2]$  at the transition point ( $C_{i-t}$ ,  $A_{n-t}$ ) on  $A/C_i$  curve) (h),  $\Phi_{PHII}$  (photochemical efficiency of photosystem II) (i),  $J_c$  (electron transport to carboxylation) (j),  $J_o$  (electron transport to oxygenation) (k) and  $g_m$  (mesophyll conductance) (l). Means ( $\pm$ SE,  $n = 6$ ) with different letters were significantly different from each other ( $P \leq 0.05$ ). See Figure 1 for other explanations.

regeneration limitation and  $ACE$  (Figure 5) but had no significant effect on  $CCP_{aci}$  (intersection of  $A/C_i$  curve and X-axis, Figure 5). The photosynthetic rate at growth  $C_a$  was lower than the transition point of photosynthetic limitation  $C_{i-t} - A_{n-t}$  in the ACT treatment (triangle at  $C_{i-ACT400}$  and  $A_{n-ACT400}$  in Figure 5a) than in the ECT treatment on (triangle at  $C_{i-ECT750}$  and  $A_{n-ECT750}$  in Figure 5b). The ratio of  $C_i$  at growth  $C_a$  and  $C_i$  at the transition point of photosynthetic limitation from RuBP carboxylation limitation to RuBP regeneration limitation and the ratio of the corresponding photosynthetic rate were both  $<1$  for the ACT treatment and  $>1$  for the ECT treatment (Figure 6), indicating that photosynthesis was limited by RuBP carboxylation under ACT but by RuBP regeneration under ECT (Figure 7).

## Discussion

### Photosynthetic limitation shifted from RuBP carboxylation to RuBP regeneration under elevated $\text{CO}_2$

The identification of specific processes or traits limiting photosynthesis is critical for understanding photosynthetic acclimation to  $\text{CO}_2$  and temperature (Busch and Sage 2017). The classical FvBC model divides the photosynthesis process into three restriction stages on the  $A/C_i$  curve: RuBP carboxylation, RuBP regeneration and TPU restrictions (Busch and Sage, 2017). Under current ambient atmospheric  $\text{CO}_2$  levels, photosynthesis is generally limited by RuBP carboxylation (Kumarathunge et al. 2019). However, the photosynthesis of C3 plants is more likely limited by RuBP regeneration under elevated  $\text{CO}_2$  levels in the future (Smith and Keenan 2020, Suzuki et al. 2021).

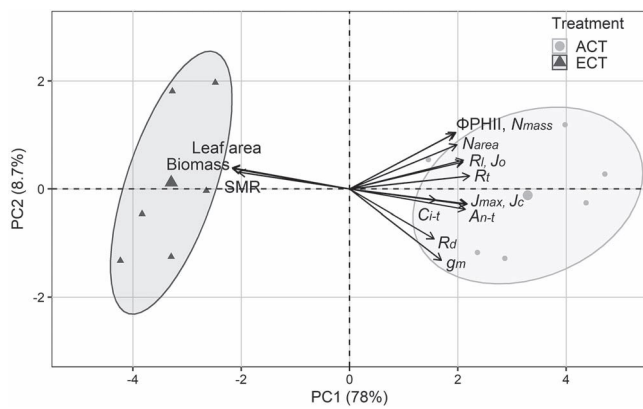


Figure 3. PCA between ACT (ambient 400  $\mu\text{mol mol}^{-1}$  CO<sub>2</sub> and temperature) and ECT (750  $\mu\text{mol mol}^{-1}$  CO<sub>2</sub> and current temperature + 4 °C) seedlings on growth and photosynthesis parameters.  $\Phi\text{PIII}$ : photochemical efficiency of photosystem II,  $N_{\text{mass}}$ : leaf N concentration,  $N_{\text{area}}$ : leaf N per unit area,  $R_i$ : photorespiration rate,  $J_o$ : electron transport to oxygenation,  $R_t$ : leaf total respiration under light,  $C_{i-t}$ : intercellular [CO<sub>2</sub>] at the transition point between Rubisco limitation and RuBP regeneration limitation based on  $A/C_i$  curve,  $J_{\text{max}}$ : maximum of photosynthetic electron transport rate,  $J_c$ : electron transport to carboxylation,  $A_{n-t}$ : net photosynthesis rate at  $C_{i-t}$ ,  $R_d$ : daytime respiration,  $J_{\text{max}}/N_{\text{area}}$ : max electron transport rate per area leaf N and  $g_m$ : mesophyll conductance.

In this study, under the ECT treatment, the photosynthesis of yellow birch seedlings was primarily limited by RuBP regeneration. The value of  $C_{i-g}/C_{i-t}$  was <1 in the ACT and >1 under the ECT treatment, indicating that the primary limitation to photosynthesis shifted from RuBP carboxylation limitation under ACT to RuBP regeneration limitation under ECT.

The transition of photosynthetic limitation provides critical insights for the better understanding of photosynthetic acclimation. However, there is generally a lack of information in the literature on the transition point (Busch and Sage 2017). The transition point may reflect the coordination between the  $J_{\text{max}}$  and  $V_{\text{cmax}}$  (related to  $J_{\text{max}}/V_{\text{cmax}}$ , Figure 7). It is generally believed that  $J_{\text{max}}$  is closely related to  $V_{\text{cmax}}$  and that changes in one cause corresponding changes in the other (Timm et al. 2016). Indeed, the ECT treatment reduced both  $J_{\text{max}}$  and  $V_{\text{cmax}}$ , but the relative effects on the two variables were different. The  $J_{\text{max}}/V_{\text{cmax}}$  ratio can represent the capacity balance between  $J_{\text{max}}$  and  $V_{\text{cmax}}$  or resources allocations within the leaf (Dusenge et al. 2021) and may be used as a diagnostic tool for the optimal net photosynthetic rate  $A_{\text{opt}}$  (Stefanski et al. 2020). Warmer temperatures tend to decrease the  $J_{\text{max}}/V_{\text{cmax}}$  ratio (Kumarathunge et al. 2019) and are related to four various patterns of  $J_{\text{max}}$  and  $V_{\text{cmax}}$  (Table 3, columns c1–c4). By contrast, elevated CO<sub>2</sub> generally increases the  $J_{\text{max}}/V_{\text{cmax}}$  (Smith and Keenan 2020) and also with four various patterns of  $J_{\text{max}}$  and  $V_{\text{cmax}}$  (Table 3, columns c5–c8). Therefore, we conclude that the warmer temperature was primarily responsible for the decline in  $J_{\text{max}}/V_{\text{cmax}}$  under ECT. However, the decline in  $g_m$  in the ECT treatment may also have contributed to the

decline in the  $J_{\text{max}}/V_{\text{cmax}}$  ratio. The reduced  $g_m$  presumably reduced CO<sub>2</sub> supply to Rubisco, leading to a lower CO<sub>2</sub>/O<sub>2</sub> ratio which favors photorespiration (Lambers and Oliveira 2019). Changes in the  $J_{\text{max}}/V_{\text{cmax}}$  ratio by warming is usually driven by photorespiration (Smith and Keenan 2020). The declines in  $J_{\text{max}}$  and  $J_{\text{max}}/V_{\text{cmax}}$  in this study are consistent with the predicted trends of responses (Table 3). A shift of primary photosynthetic limitation from  $V_{\text{cmax}}$ -related carboxylation to  $J_{\text{max}}$ -related RuBP regeneration restriction may lead to the adjustment of plant metabolic mode and the application of  $V_{\text{cmax}}$ -based models.

### Photosynthetic capacity versus photosynthetic rate

Photosynthetic capacity is the potential maximum rate of photosynthesis, while the actual rate of photosynthesis is the portion of the photosynthetic capacity that is realized under specific physiological and environmental conditions, such as the availability of substrates, the activation state of enzymes activation, light, temperature, etc. (Stefanski et al. 2020). About half of leaf nitrogen is directly related to photosynthesis, 20% of which is directly related to Rubisco, and the insufficient supply of nitrogen will decrease the photosynthetic capacity ( $V_{\text{cmax}}$  and  $J_{\text{max}}$ ) (Silva-Pérez et al. 2020). Elevated CO<sub>2</sub> increases plant biomass, dilutes leaf nitrogen concentration and leads to reductions in photosynthetic capacity (Byeon et al. 2021).

The CO<sub>2</sub> acts both to activate the Rubisco enzyme and as a substrate of Rubisco carboxylation, and thus increases in CO<sub>2</sub> concentration can increase the efficiency of carboxylation (Smith and Keenan 2020). Therefore, a decline in photosynthetic capacity in response to elevated CO<sub>2</sub> does not necessarily lead to a reduction in the photosynthetic rate (Way et al. 2015, Stefanski et al. 2020). Indeed, the photosynthetic rate of yellow birch in this study was significantly higher in the ECT than in the ACT treatment.

### Source and sink limitation

There was a dichotomy between whether tree carbon sequestration is carbon source limited (limited by how much carbon the plant can photosynthesize) or sink limited (limited by how much the plant can grow because of all environmental factors; Green and Keenan 2022). Our results show that the domestication of yellow birch to ECT treatment conforms to the relationship between carbon source versus carbon sink. It is believed that elevated CO<sub>2</sub> reduces substrate limitation to RuBP carboxylation and acclimated plants divert resource allocation from CO<sub>2</sub> sequestration to other productivity-limiting processes (Smith and Keenan 2020). Even if more carbon is available to vegetation, other factors (like temperature, light, nutrients and water) are needed to help stoke growth from photosynthesis (Green and Keenan 2022). We found that the leaf area appears to bridge the carbon source and sink in yellow birch to ECT. Both PCA and correlation analysis found that



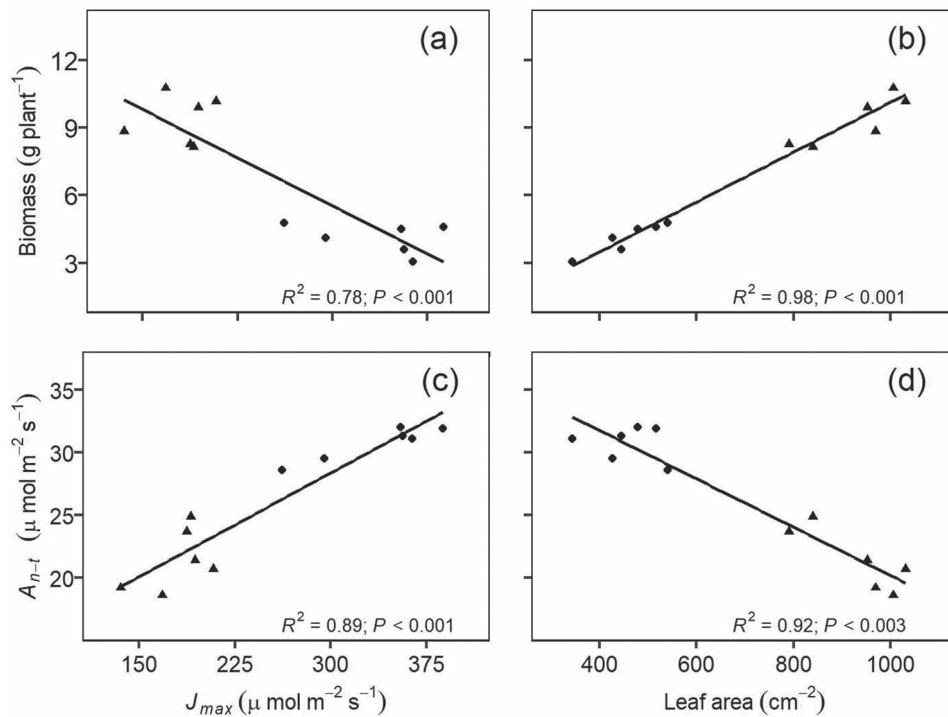


Figure 4. Relationship between biomass and  $J_{max}$  (a), leaf area (b), between  $A_{n-t}$  and  $J_{max}$  (c) and leaf area (d). Triangles represent the ACT-treated seedlings and the diamonds are ECT-treated seedlings. See Figure 1 and Table 1 for further details.

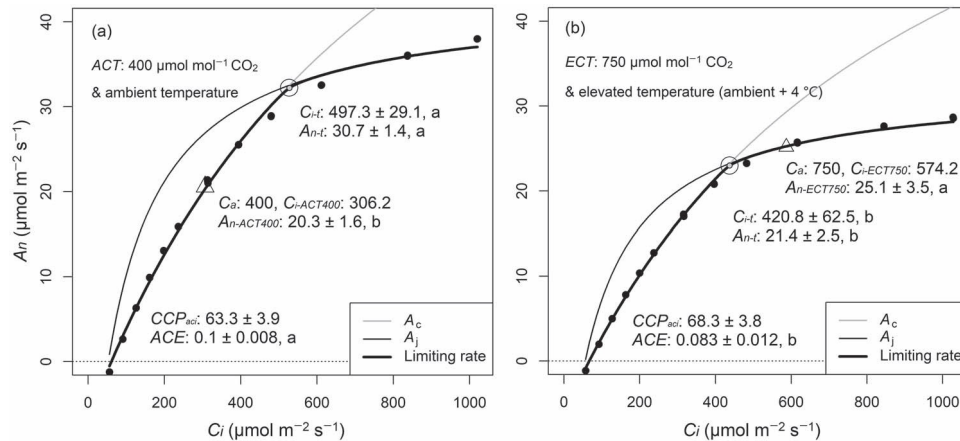


Figure 5.  $A/C_i$  curves of yellow birch seedlings grown under ACT (a) and ECT (b). Each solid dot represents the means of six ( $C_i$ ,  $A_n$ ) values. The circles denote the transition point ( $C_{i-t}$ ,  $A_{n-t}$ ) of the photosynthesis limitation from Rubisco activity to RuBP regeneration as determined by the findCiTransition function in the plantecophys R package. The triangles mark the photosynthetic rates ( $C_{i-g}$ ,  $A_{n-g}$ ) under growth  $C_a$  (400 vs 750). ACE: ACE estimated from the initial slope of  $A/C_i$  curve;  $CCP_{aci}$ :  $CO_2$  compensation point estimated from the  $A/C_i$  curve intersecting point on X-axis.  $A_n$  with different letters in the same figure are significantly different from each other ( $P \leq 0.05$ ). See Table 1 for further details.

the leaf area was closely related to biomass. The increases in biomass and growth in turn can increase the strength of carbon sinks and thus demand photosynthetic products. Furthermore, the increases in the amount of stem (i.e., stem mass ratio (SMR)) and leaves (i.e., canopy size) can further enhance light capture and  $CO_2$  sequestration (Slot and Winter 2017). ECT treatment seems to promote yellow birch carbon sink demand intensity furthermore maximizing carbon gain. We would like to

point out that the seedlings in this study were provided with optimal levels of fertilizers, particularly nitrogen. Trees grown in the field, however, are generally much more limited by the low nitrogen supply than the seedlings in this study. Therefore, we speculate that the degrees of photosynthetic downregulation and leaf area increase would be greater if trees in the field were exposed to the same degree of  $CO_2$  elevation and warming as the treatments used in the study.



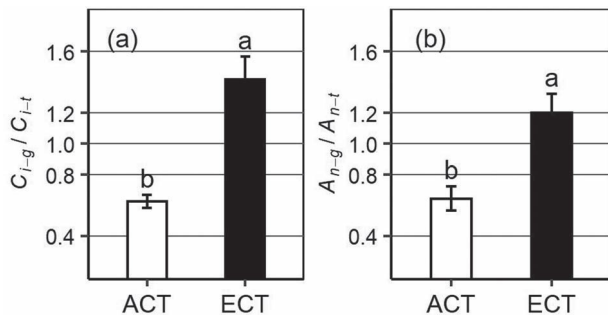


Figure 6. Effects of CT treatments on the ratio of intercellular CO<sub>2</sub> concentration at growth  $C_a$  ( $C_{i-g}$ ) and that at the transition point ( $C_{i-t}$ ) of photosynthesis limitation from Rubisco activity to RuBP regeneration (a) and the ratio of the photosynthetic rate at growth  $C_a$  ( $A_{n-g}$ ) and the photosynthetic rate at the transition point ( $A_{n-t}$ ) of photosynthesis limitation from Rubisco activity to RuBP regeneration (b). A value  $< 1$  indicates that photosynthesis was limited by RuBP carboxylation limitation, while a value  $> 1$  means that it was limited by RuBP regeneration limitation. Means ( $\pm$ SE,  $n = 6$ ) with different letters were significantly different from each other ( $P \leq 0.05$ ).

### Electron distribution and respiration

The decrease in  $J_{max}$  was the primary contributor to the decline in  $J_{max}/V_{cmax}$  in yellow birch seedlings under ECT as  $V_{cmax}$  also declined ( $73.9 \pm 5.6 \mu\text{mol m}^{-2} \text{s}^{-1}$  in ACT vs  $65.5 \pm 4.6 \mu\text{mol m}^{-2} \text{s}^{-1}$  in ECT, not statistically significant). It should be noted that  $J_{max}$  and  $V_{cmax}$  normalized by  $N_{area}$  ( $J_{max}/N_{area}$  and  $V_{cmax}/N_{area}$ ) showed opposite response patterns to treatment, suggesting that nitrogen may have been involved in the photosynthetic acclimation process. The ECT significantly reduced the partitioning of electron flow to carboxylation ( $J_c$ ) and oxidation ( $J_o$ , related to photorespiration), while  $J_c/J_o$  did not change significantly. Since  $J_{max}$ ,  $J_c$  and  $A_{n-t}$  were clustered together (high correlation) in PCA (Figure 3), the electron flow to carboxylation may be the key factor influencing the shift of primary photosynthetic limitation (Chang et al. 2016).

Respiration, both daytime respiration ( $R_d$ ) and photorespiration ( $R_i$ ) can affect the carbon balance of plants. The  $R_i$  consumes reductant equivalents produced by the electron transport chain, and  $R_d$  provides carbon skeletons for nitrogen assimilation (Tcherkez et al. 2017). Our results that ECT reduced  $R_d$  and  $R_i$  in yellow birch are consistent with the literature (Dusenge et al. 2019, Birami et al. 2020).

### Conclusions

In conclusion, photosynthetic acclimation caused by elevated CO<sub>2</sub> is widespread in plants. Our results suggest that the following two aspects are very important to understand this phenomenon: first, although the photosynthetic parameters per unit leaf area decreased, the increase of leaf area more than offset the effect of the photosynthetic downregulation, resulting

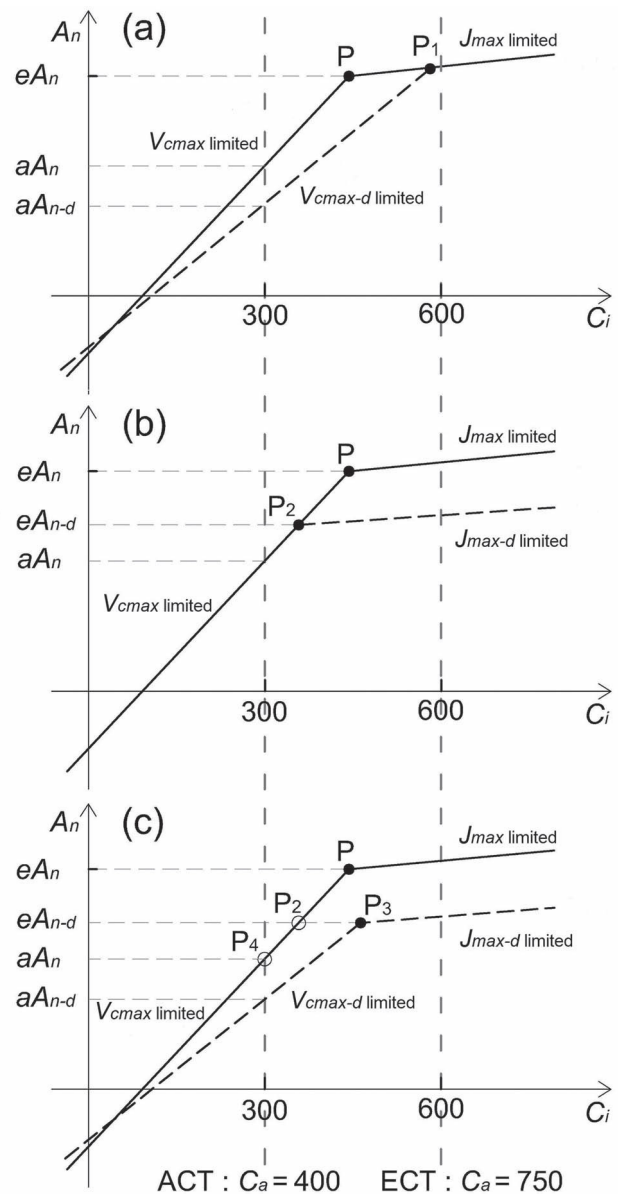


Figure 7. Conceptual diagram showing relationships between the transition point (solid circle, ( $C_{i-t}$ ,  $A_{n-t}$ )) of photosynthetic limitation from Rubisco activity to RuBP regeneration and photosynthetic rate (empty circle) at growth  $C_a$ . In (a), the operating  $C_i$  was assumed to be  $300 \mu\text{mol mol}^{-1}$  (close to the measured operating  $C_i$ ) for seedlings grown under ACT ( $C_a = 400 \mu\text{mol mol}^{-1}$ ) and as  $600 \mu\text{mol mol}^{-1}$  for seedlings grown under ECT ( $C_a = 750 \mu\text{mol mol}^{-1}$ ); P was the transition point of photosynthetic limitation from Rubisco activity to RuBP regeneration limitation (the co-limitation stage has been simplified); the dashed line represents Rubisco limited photosynthetic rates, while the second section of the solid line represents RuBP regeneration limited photosynthetic rates. Regardless of whether  $V_{cmax}$  decreased and  $J_{max}$  remained constant (black dashed line in (a)) or  $V_{cmax}$  remained constant and  $J_{max}$  decreased (dark dashed line in (b)), or both  $V_{cmax}$  and  $J_{max}$  decreased (dark dashed line in (c)), the photosynthesis of seedlings grown under ECT was restricted by  $J_{max}$ . Decreases in  $V_{cmax}$  can lead to increases in  $C_{i-t}$ , while decreases in  $J_{max}$  lead to decreases in both  $C_{i-t}$  and  $A_{n-t}$ . The subscript 'd' indicates a drop, the prefix 'e' represents ECT and 'a' represents ACT. Solid circles indicate the transition point of photosynthetic restriction. Circle P2 and circle P4 in (c) represent the photosynthetic rate at growth CO<sub>2</sub> ( $eA_{n-d}$  for ECT,  $aA_n$  for ACT).

Table 3. Four possible various patterns of  $J_{max}$  and  $V_{cmax}$  to  $J_{max}/V_{cmax}$  affected by elevated temperature (columns c1–c4) or CO<sub>2</sub> (columns c5–c8).

	Elevated temperature reduced $J_{max}/V_{cmax}$				Elevated CO <sub>2</sub> increased $J_{max}/V_{cmax}$			
	c1	c2	c3	c4	c5	c6	c7	c8
$J_{max}$	↓	↔	↓	↑	↑	↔	↓	↑
$V_{cmax}$	↔	↑	↓	↑	↔	↓	↓	↑

Note: The arrows '↔', '↑', and '↓' mean constant, increase and decrease, respectively; the size of the symbol represents the degree of change.

in increased biomass production at the whole-plant level under elevated CO<sub>2</sub> and warmer temperature; second, elevated CO<sub>2</sub> and warmer temperature promoted the shift of photosynthetic restriction from RuBP carboxylation to RuBP regeneration, which drove the changes in biochemical processes of the photosynthetic apparatus. Under RuBP regeneration limitation, the photosynthetic rate was mainly determined by  $J_{max}$ . Therefore, models and conclusions based on  $V_{cmax}$  alone should be adjusted for the elevations in CO<sub>2</sub> and temperature in the future.

### Supplementary data

The dataset generated for this study is available as supplementary data at *Tree Physiology* Online.

### Acknowledgments

We want to thank Ms Keri Pidgen, the Greenhouse Manager, for her logistic support and other operational assistance during the experiments.

### Funding

The study was supported by a Natural Sciences and Engineering Research Council of Canada (NSERC) Discovery Development Grant to Q.-L.D. (Project No. DDG-2020-00008).

### Conflict of interest

The authors declare no conflict of interest.

### References

- Ainsworth EA, Long SP (2005) What have we learned from 15 years of free-air CO<sub>2</sub> enrichment (FACE)? A meta-analytic review of the responses of photosynthesis, canopy properties and plant production to rising CO<sub>2</sub>. *New Phytol* 165:351–372.
- Ainsworth EA, Long SP (2021) 30 years of free-air carbon dioxide enrichment (FACE): What have we learned about future crop productivity and its potential for adaptation? *Glob Chang Biol* 27:27–49.
- Anderson-Teixeira KJ, Miller AD, Mohan JE, Hudiburg TW, Duval BD, DeLucia EH (2013) Altered dynamics of forest recovery under a changing climate. *Glob Chang Biol* 19:2001–2021.

- Apgaua DMG, Tng DYP, Forbes SJ, Ishida YF, Vogado NO, Cernusak LA, Laurance SGW (2019) Elevated temperature and CO<sub>2</sub> cause differential growth stimulation and drought survival responses in eucalypt species from contrasting habitats. *Tree Physiol* 39:1806–1820.
- Birami B, Nägele T, Gattmann M, Preisler Y, Gast A, Arneith A, Ruehr NK (2020) Hot drought reduces the effects of elevated CO<sub>2</sub> on tree water-use efficiency and carbon metabolism. *New Phytol* 226:1607–1621.
- Busch FA, Sage RF (2017) The sensitivity of photosynthesis to O<sub>2</sub> and CO<sub>2</sub> concentration identifies strong Rubisco control above the thermal optimum. *New Phytol* 213:1036–1051.
- Byeon S, Song W, Park M et al. (2021) Down-regulation of photosynthesis and its relationship with changes in leaf N allocation and N availability after long-term exposure to elevated CO<sub>2</sub> concentration. *J Plant Physiol* 265:153489. <https://doi.org/10.1016/j.jplph.2021.153489>.
- Chang CY, Fréchette E, Unda F, Mansfield SD, Ensminger I (2016) Elevated temperature and CO<sub>2</sub> stimulate late-season photosynthesis but impair cold hardening in Pine. *Plant Physiol* 172:802–818.
- Chavan SG, Duursma RA, Tausz M, Ghannoum O (2019) Elevated CO<sub>2</sub> alleviates the negative impact of heat stress on wheat physiology but not on grain yield. *J Exp Bot* 70:6447–6459.
- Cox RM, Zhu XB (2003) Effects of simulated thaw on xylem cavitation, residual embolism, spring dieback and shoot growth in yellow birch. *Tree Physiol* 23:615–624.
- Delagrange S, Messier C, Lechowicz MJ, Dizengremel P (2004) Physiological, morphological and allocational plasticity in understory deciduous trees: importance of plant size and light availability. *Tree Physiol* 24:775–784.
- Dusenge ME, Duarte AG, Way DA (2019) Plant carbon metabolism and climate change: elevated CO<sub>2</sub> and temperature impacts on photosynthesis, photorespiration and respiration. *New Phytol* 221:32–49.
- Dusenge ME, Madhavji S, Way DA (2020) Contrasting acclimation responses to elevated CO<sub>2</sub> and warming between an evergreen and a deciduous boreal conifer. *Glob Chang Biol* 26:3639–3657.
- Dusenge ME, Witemann M, Mujawamariya M et al. (2021) Limited thermal acclimation of photosynthesis in tropical montane tree species. *Glob Chang Biol* 27:4860–4878.
- Duursma RA (2015) Plantecophys—an R package for analysing and modelling leaf gas exchange data. *PLoS One* 10:e0143346. <https://doi.org/10.1371/journal.pone.0143346>.
- Farquhar GD, von Caemmerer JA, Berry JA, Berry (1980) A biochemical model of photosynthetic CO<sub>2</sub> assimilation in leaves of C<sub>3</sub> species. *Planta* 149:78–90.
- Green JK, Keenan TF (2022) The limits of forest carbon sequestration. *Science* 376:692–693.
- Inoue S, Dang QL, Man R, Tedla B (2019) Northward migration of trembling aspen will increase growth but reduce resistance to drought-induced cavitation in the xylem. *Botany* 97:627–638.

- IPCC (2021) Climate change 2021: the physical science basis. Contribution of working Group I to the sixth assessment report of the intergovernmental panel on climate change. Cambridge University Press, Cambridge, United Kingdom and New York, NY, USA.
- Jayawardena DM, Heckathorn SA, Bista DR, Boldt JK (2019) Elevated carbon dioxide plus chronic warming causes dramatic increases in leaf angle in tomato, which correlates with reduced plant growth. *Plant Cell Environ* 42:1247–1256.
- Kumarathunge DP, Medlyn BE, Drake JE, Rogers A, Tjoelker MG (2019) No evidence for triose phosphate limitation of light-saturated leaf photosynthesis under current atmospheric CO<sub>2</sub> concentration. *Plant Cell Environ* 42:3241–3252.
- Kurepin LV, Stangl ZR, Ivanov AG, Bui V, Mema M, Hüner NPA, Öquist G, Way D, Hurrey V (2018) Contrasting acclimation abilities of two dominant boreal conifers to elevated CO<sub>2</sub> and temperature. *Plant Cell Environ* 41:1331–1345.
- Lambers H, Oliveira RS (2019) *Plant physiological ecology*, 3rd edn. Springer, New York, p 736. <https://doi.org/10.1007/978-3-030-29639-1>.
- Lavoie J-M, Stevanovic T (2005) Variation of chemical composition of the lipophilic extracts from yellow birch (*Betula alleghaniensis*) foliage. *J Agric Food Chem* 53:4747–4756.
- Long SP, Ainsworth EA, Rogers A, Ort DR (2004) Rising atmospheric carbon dioxide: plants FACE the future. *Annu Rev Plant Biol* 55:591–628.
- Mathan J, Singh A, Jathar V, Ranjan A (2021) High photosynthesis rate in the selected wild rice is driven by leaf anatomy mediating high Rubisco activity and electron transport rate. *J Exp Bot* 72:7119–7135.
- Momayyezi M, Guy RD (2017) Substantial role for carbonic anhydrase in latitudinal variation in mesophyll conductance of *Populus trichocarpa* Torr. & Gray. *Plant Cell Environ* 40:138–149.
- Noyce GL, Kirwan ML, Rich RL, Megonigal JP (2019) Asynchronous nitrogen supply and demand produce nonlinear plant allocation responses to warming and elevated CO<sub>2</sub>. *Proc Natl Acad Sci USA* 116:21623–21628.
- Pastore MA, Lee TD, Hobbie SE, Reich PB (2019) Strong photosynthetic acclimation and enhanced water-use efficiency in grassland functional groups persist over 21 years of CO<sub>2</sub> enrichment, independent of nitrogen supply. *Glob Chang Biol* 25:3031–3044.
- Peter CH, Francesco L, Di Giorgio M, Thomas DS (1992) Theoretical considerations when estimating the mesophyll conductance to CO<sub>2</sub> flux analysis of the response of photosynthesis to CO<sub>2</sub>. *Plant Physiol* 98:1429–1436.
- Ross MD, Timothy JB, Florian AB, Graham DF (2020) Optimization can provide the fundamental link between leaf photosynthesis, gas exchange and water relations. *Nat Plants* 6:1116–1125.
- Salazar-Parra C, Aranjuelo I, Pascual I et al. (2015) Carbon balance, partitioning and photosynthetic acclimation in fruit-bearing grapevine (*Vitis vinifera* L. cv. Tempranillo) grown under simulated climate change (elevated CO<sub>2</sub>, elevated temperature and moderate drought) scenarios in temperature gradient greenhouses. *J Plant Physiol* 174:97–109.
- Silva-Pérez V, de Faveri J, Molero G, Deery DM, Condon AG, Reynolds MP, Evans JR, Furbank RT (2020) Genetic variation for photosynthetic capacity and efficiency in spring wheat. *J Exp Bot* 71:2299–2311.
- Slot M, Winter K (2017) Photosynthetic acclimation to warming in tropical forest tree seedlings. *J Exp Bot* 68:2275–2284.
- Slot M, Rifai SW, Winter K (2021) Photosynthetic plasticity of a tropical tree species, *Tabebuia rosea*, in response to elevated temperature and CO<sub>2</sub>. *Plant Cell Environ* 44:2347–2364.
- Smith NG, Keenan TF (2020) Mechanisms underlying leaf photosynthetic acclimation to warming and elevated CO<sub>2</sub> as inferred from least-cost optimality theory. *Glob Chang Biol* 26:5202–5216.
- Stefanski A, Bermudez R, Sendall KM, Montgomery RA, Reich PB (2020) Surprising lack of sensitivity of biochemical limitation of photosynthesis of nine tree species to open-air experimental warming and reduced rainfall in a southern boreal forest. *Glob Chang Biol* 26:746–759.
- Suzuki Y, Ishiyama K, Sugawara M et al. (2021) Overproduction of chloroplast glyceraldehyde-3-phosphate dehydrogenase improves photosynthesis slightly under elevated CO<sub>2</sub> conditions in rice. *Plant Cell Physiol* 62:156–165.
- Tcherkez G, Gauthier P, Buckley TN et al. (2017) Leaf day respiration: low CO<sub>2</sub> flux but high significance for metabolism and carbon balance. *New Phytol* 216:986–1001.
- Timm S, Florian A, Fennie AR, Bauwe H (2016) The regulatory interplay between photorespiration and photosynthesis. *J Exp Bot* 67:2923–2929.
- Tomeo NJ, Rosenthal DM (2018) Photorespiration differs among *Arabidopsis thaliana* ecotypes and is correlated with photosynthesis. *J Exp Bot* 69:5191–5204.
- Valentini R, Epron D, De Angelis P, Matteucci G, Dreyer E (1995) In situ estimation of net CO<sub>2</sub> assimilation, photosynthetic electron flow and photorespiration in Turkey oak (*Q. cerris* L.) leaves: diurnal cycles under different levels of water supply. *Plant Cell Environ* 18:631–640.
- Way DA, Oren R, Kroner Y (2015) The space-time continuum: the effects of elevated CO<sub>2</sub> and temperature on trees and the importance of scaling. *Plant Cell Environ* 38:991–1007.
- Yin X, Schapendonk AHCM, Struik PC (2019) Exploring the optimum nitrogen partitioning to predict the acclimation of C<sub>3</sub> leaf photosynthesis to varying growth conditions. *J Exp Bot* 70:2435–2447.
- Zhang H, Zhou J-F, Kan Y et al. (2022) A genetic module at one locus in rice protects chloroplasts to enhance thermotolerance. *Science* 376:1293–1300.
- Zhou H, Xu M, Pan H, Yu X (2015) Leaf-age effects on temperature responses of photosynthesis and respiration of an alpine oak, *Quercus aquifolioides*, in southwestern China. *Tree Physiol* 35:1236–1248.